Journal of the Korean Physical Society, Vol. 77, No. 5, September 2020, pp. 344∼350

Commissioning Status of the Linac for the Facility for Rare Isotope Beams

S. Lidia,* H. Ao, B. Barnes, R. Bennett, E Bernal-Ruiz, G. Bollen, J. Brandon, B. Bull, N. Bultman, F. Casagrande, D. Chabot, S. Cogan, C. Compton, K. Davidson, E. Daykin, D. Georgiobani, P. Gibson, I. Grender, S.-H. Kim, W. Hartung, M. Hausmann, L. Hodges, K. Holland, A. Hussain, M. Ikegami, M. Konrad, G. Kiupel, T. Larter, Z. Li, I. Malloch, G. Machicoane, H. Maniar, P. Manwiller, B. Martins, T. Maruta, D. Morris, P. Morrison, C. Morton, I. Nesterenko, D. Omitto, P. Ostroumov, F. Pellemoine, A. Plastun, J. Popielarski, L. Popielarski, E. Pozdeyev, H. Ren, P. Rodriguez, S. Rodriguez, T. Russo, K. Saito, R. Shane, S. Stanley, A. Stolz, G. Timko, J. Wei, M. Xu, T. Xu, Y. Yamazaki, T. Yashimoto, Q. Zhao and S. Zhao

Facility for Rare Isotope Beams, Michigan State University, East Lansing, MI 48824, USA

(Received 8 January 2020; accepted 20 February 2020)

The Facility for Rare Isotope Beams will be completed in late 2021. We report here on the current efforts to commission the first stages of the 200-MeV/u superconducting, continuous wave heavy-ion linac. The statuses of the cryogenic plant and its distribution system, the accelerator cryomodule commissioning and operations, the ion source and front end transport development, the radio-frequency quadrupole commissioning, and thenbeam dynamics development to support high-power operation are reviewed. Plans for commissioning the remainder of the linac systems are presented.

Keywords: Linear accelerator, Commissioning, Superconducting RF, Heavy Ion
DOI: 10.3938/jkps.77.344

I. INTRODUCTION

The Facility for Rare Isotope Beams (FRIB) is a high-power heavy-ion accelerator facility presently under construction and commissioning at Michigan State University in the USA. The FRIB is a power frontier accelerator facility aiming to provide two to three orders of magnitude higher beam power than existing heavy-ion accelerator facilities. The FRIB linac is designed to accelerate all stable ions to energies above 200 MeV/u with a beam power of up to 400 kW with continuous wave (CW) operation [1]. The FRIB linac is being constructed beside the existing National Superconducting Cyclotron Laboratory (NSCL) to utilize its experimental beamlines (see Fig. 1). While the linac tunnel is located about 10 m below ground level for radiation shielding, its front end with two electron cyclotron resonance (ECR) ion sources [2] is located at ground level. This layout allows us to develop the next ion beam with an independent source while simultaneously providing a beam for user operation. The 12-keV/u heavy-ion beams extracted from the ion sources are delivered to a 80.5-MHz normal conducting radio-frequency quadrupole (RFQ) linac situated in the linac tunnel with a low-energy beam transport (LEBT) beamline. The LEBT has various instrumentation including extensive beam diagnostics, a pulsed electrostatic chopper and beam attenuators [3]. While the FRIB linac operates in the CW mode, the chopper allows pulsed beam operation for commissioning and tuning. As a high-power accelerator, mitigating excess beam loss during commissioning is important, and the chopper and beam attenuators play key roles to this end.

A characteristic feature of the FRIB linac is extensive adoption of superconducting RF technology [4]. The heavy-ion beams accelerated to 0.5 MeV/u with the RFQ are injected into superconducting RF (SRF) cavities in the first linac segment, or LS1. The LS1 has two types of 80.5-MHz quarter wave resonators (QWRs) with geometrical beta, or β, of 0.041 and 0.085. Then, the beam is accelerated with 322-MHz half wave resonators (HWRs) with $\beta = 0.29$ and $\beta = 0.53$ in the second linac segment, or LS2, and then further accelerated with 322-MHz HWRs with $\beta = 0.53$ in the third linac segment, or LS3. The total number of SRF cavities is 324, and they are distributed to 46 cryomodules.

The beams accelerated with LS3 are delivered to the production target with a beam delivery system (BDS) to produce rare-isotope beams as secondary beams for user experiments. The FRIB linac has four beam dumps and three low-power beam stops to allow segment-by-segment tuning. A straight beam dump and a 45-degree beam dump are located in the first folding segment, or

*E-mail: lidia@frib.msu.edu

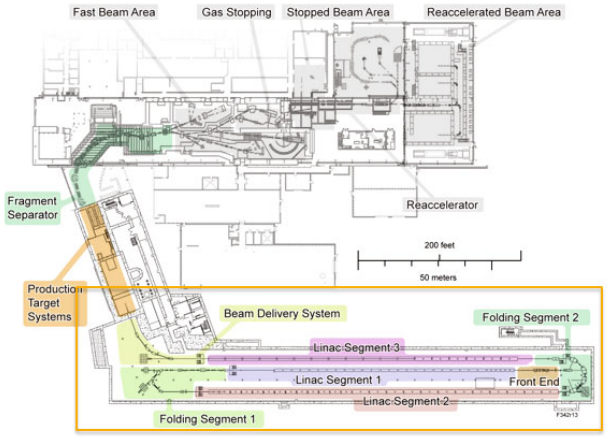

Fig. 1. Layout of the Facility for Rare Isotope Beams, showing the superconducting linac and production target systems, fragment separator, and experimental beamlines.

Fig. 2. Elements of the FRIB cryogenic system: (left) 4.5-K cold box, (middle) warm compressor, (right) tunnel transfer lines.

FS1, for the tuning of LS1. Two straight dumps are located at the second folding segment, or FS2, and the BDS for the tuning of LS2 and LS3, respectively. The straight and the 45-degree beam dumps in FS1 have average beam power capacities of 15 W and 500 W, respectively, and the beam dumps in FS2 and BDS have average beam power capacities of 150 W. The beam commissioning and tuning are conducted within those beam power capacity restrictions. Current beam commissioning activities are underway in the front end, LS1, and FS1 segments.

II. CONSTRUCTION AND INSTALLATION STATUSES

The cryogenic system has been installed and commissioned [5] to support total linac operations. The 4.5-K cold box (see Fig. 2) has been in operation since 2018. All 46 cryogen transfer line sections have been installed in the tunnel, and have been in with full operation since September 2019. Linac segments LS1 and LS2 cryogen distribution at 2 K has been established in individual and combined operation. A dedicated cryo-control room and cryo-network are fully operational and have supported

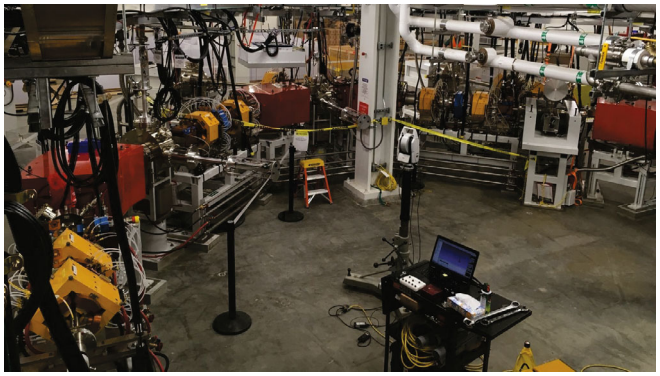

Fig. 3. Folding segment 1 installation is completed.

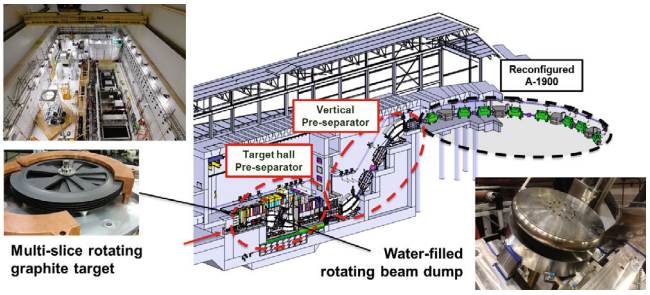

Fig. 4. Production target facility and fragment separator beamline.

the step-wise commissioning of each sub-system, as well as the operation of the commissioned systems.

All LS1 and LS2 cryomodules have been installed and cooled to operating temperatures. This incorporates 3 $\beta = 0.041$ and 11 $\beta = 0.085$ accelerating modules, and 1 $\beta = 0.085$ matching module, operating at 4.5 K in LS1 and 12 $\beta = 0.29$ and 12 $\beta = 0.53$ accelerating modules operating at 2 K in LS2. The remaining 6 $\beta = 0.53$ accelerating modules for LS3 are completing installation in the tunnel. All cryomodule cavity systems have been commissioned to higher than required acceleration gradients at 2 K: 5.1 MV/m for $\beta = 0.041$ QWRs, 5.5 MV/m for $\beta = 0.085$, 7.7 MV/m for $\beta = 0.29$ and 7.7 MV/m for $\beta = 0.53$.

Folding segment FS1 has completed installation and is being readied for beam operations (see Fig. 3). Folding Segment FS2 is under construction as the superconducting dipole magnets are currently in fabrication. Installation of warm transport vacuum chambers, diagnostic boxes, and quadrupole magnets following the LS3 cryomodules is nearing completion.

The production target facility and fragment separator are currently on track for installation (see Fig. 4). The target facility provides shielding for 400-kW heavy-ion beam operation. Large vacuum chambers are installed to accommodate the target, beam dump, wedge, and vertical preseparator beamline. Remote handling systems are in use for installation activities, and non-conventional utilities are installed. The existing A1900 separator

Table 1. Commissioning stages for the FRIB accelerator and the rare isotope production facilities.

Stage	Scope	Date Completed
1	Ion Source, Low Energy Beam Transport (LEBT), Medium Energy Beam Transport (MEBT)	July 2017
2	Linac Segment (LS) 1 ($\beta = 0.041$ cryomodules)	May 2018
3	Rest of LS1 and the First Dipole of the Folding Segment (FS) 1	February 2019
4	Rest of FS1, LS2, and Part of FS2 to the Straight Dump	
5	Rest of FS2, LS3, and Part of BDS to the Straight Dump	
6	Rest of BDS, Target Hall Pre-separator	
7	Complete All Prior Post-start Items, Entire Facility Readiness	

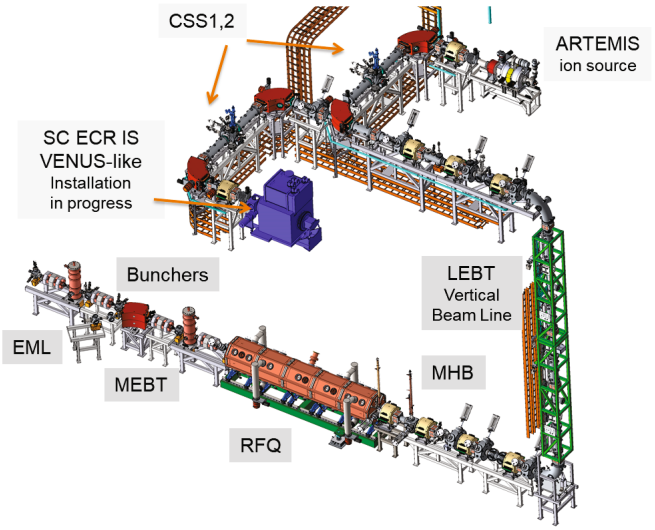

Fig. 5. FRIB front-end ion source, beam transport, RFQ accelerator, and matching optics layout.

beamline, part of the current experimental physics facility, is in the final design and planning stages for reconfiguration service isotope selection from the FRIB target facility.

III. ACCELERATOR SYSTEMS' COMMISSIONING

FRIB accelerator systems have been undergoing phased commissioning to establish key performance parameters and operating envelopes. The stages are listed in Table 1. The FRIB front end system layout is shown in Fig. 5. The beamline consists of two, independent ECR ion sources the 14-GHz, room-temperature ARTEMIS, currently in operation, and the 28-GHz, superconducting VENUS, currently being installed. The 12-keV/u low-energy beam transport (LEBT) line hosts the electrostatic chopper, electrostatic quadrupoles and bends, magnetic solenoids, multi-harmonic buncher (40.25, 80.5, 120.75 MHz) [6], beam attenuators, and diagnostic systems [3]. The CW RFQ operates at 500 keV/u with a capture efficiency >85% [6]. The medium energy beam transport (MEBT) line holds two 100-kV, 80.5-MHz bunching cavities, a 45-degree dipole and energy measurement line (EML), and magnetic quadrupole focusing elements. Beam instrumentation and diagnostic systems include multiple Faraday cups, view screens, and wire profile monitors in the LEBT and the MEBT sections, and AC-coupled beam current monitors and narrowband beam position monitors in the lower LEBT and MEBT sections. The charge selection system (CSS) vacuum chamber holds vertical and horizontal slit systems, Faraday cup, view screen, and vertical and horizontal Allison scanners for beam phase-space measurements. The electrostatic chopper and the beam attenuation systems have been commissioned and provide control over the beam time structure and over the average and the peak beam powers [7].

The front end systems were successfully commissioned in 2017 [8], including conditioning the RFQ to 50-kW CW operation and acceleration of $^{40}Ar^{9+,10+}$, and $^{86}Kr^{17+,18+}$. Average currents up to ~250 eμA have been produced for argon beams. Subsequent conditioning of the RFQ has raised the upper power limit to >100 kW, sufficient for acceleration of uranium ion beams (Q/A ~ 1/7). No multipacting was observed for RF powers over 20 kW, at vacuum levels better than 1×10^{-7} Torr during conditioning. X-ray radiation levels < 0.1 mRad/hour at a 102-kW CW RF power input were measured at a 50-cm distance.

Beam transport and optimization studies following initial commissioning activities concentrated on several tasks [9]:

- Evaluation of the beam rms parameters and emittance from measured data;
- Beam optics tuning to create a small horizontal beam size in the charge selection slits;
- Beam-based alignment of beam diagnostics devices, such as image viewers, the Allison scanners and profile monitors;
- Minimization of transverse emittance growth due to X-Y coupling of the non-axially symmetric beam;

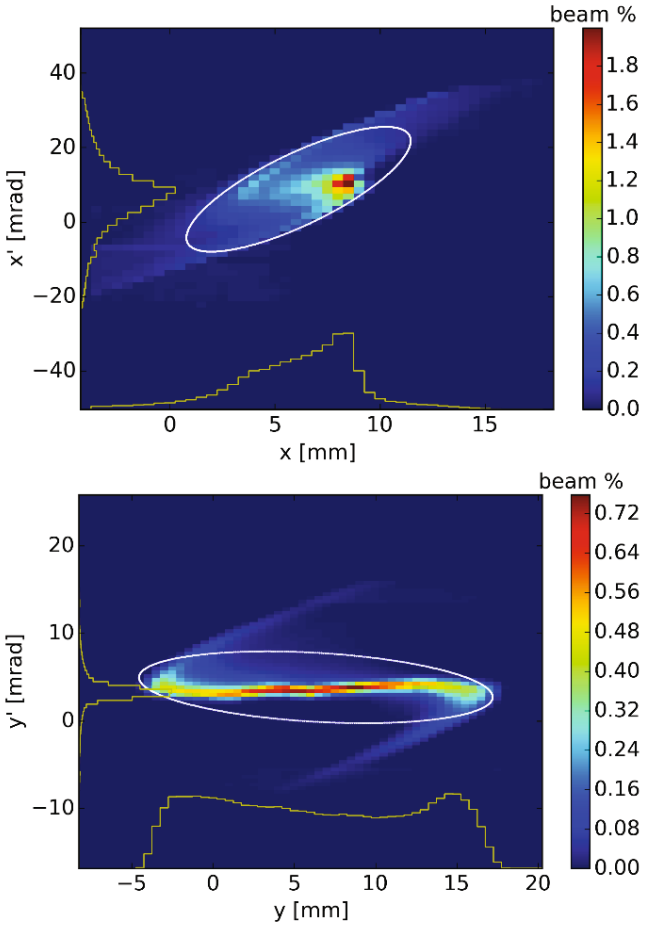

Fig. 6. Typical phase-space distributions measured with the Allison scanner (argon 50 eμA).

- Beam central trajectory correction along the LEBT;
- Beam matching into the RFQ transverse acceptance;
- Transport of a dual-charge-state krypton beam and matching to the RFQ.

Typical phase-space measurements in the CSS are shown in Fig. 6. Reconstruction of beam envelopes from profile monitor measurements along the LEBT beamline up to the RFQ show excellent consistency with design. Typical measured normalized rms emittances are 0.131π mm-mrad and 0.125π mm-mrad in the horizontal and the vertical planes, respectively, for ∼50-eμA argon beams.

The LEBT is designed to transport dual-charge-state heavy ion beams in order to increase overall beam intensities. To test this feature, we have selected a dual-charge-state krypton beam, $^{86}Kr^{17+}$ and $^{86}Kr^{18+}$, from the ion source. With appropriate Q/A scaling of the transport optics, this dual-charge-state krypton beam was transported with nearly 100% efficiency to the entrance of the RFQ. The intensities of $^{86}Kr^{17+}$ and $^{86}Kr^{18+}$ were 33 eμA and 27 eμA, respectively.

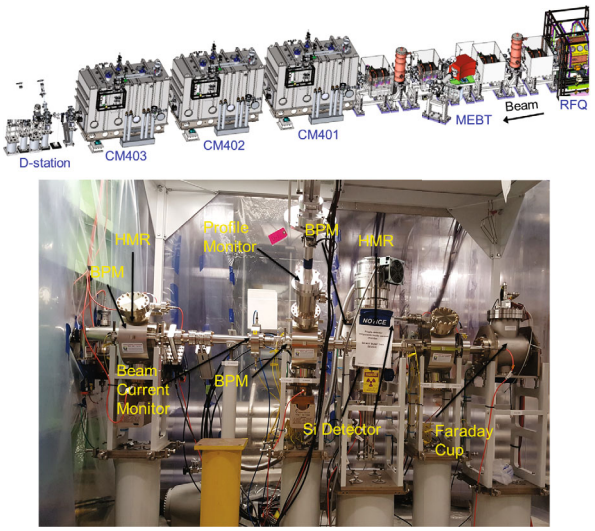

Fig. 7. (Top) Beamline for initial linac commissioning. (Bottom) A temporary diagnostic station ('D-station') has been installed in place of the first $\beta = 0.085$ cryomodule. The locations of beam position monitors (BPM), beam current monitors (BCM), halo monitoring rings (HMR), silicon detector (SiD), profile monitor (PM), and Faraday cup (FC) are indicated.

1. Linac Segment Commissioning

Commissioning the first linac segment (LS1) was accomplished in two stages. The first stage was comprised of the three $\beta = 0.041$ cryomodules, with the first $\beta = 0.085$ cryomodule having been temporarily replaced with a commissioning diagnostic station, as shown in Fig. 7. The primary goals during this stage were (i) confirmation of the accelerator design and required functionality, (ii) detailed study of accelerated beam parameters, (iii) demonstration of the highest beam energy (with available accelerating gradients) in the first three cryomodules, and (iv) demonstration of high-power equivalent beam in a pulsed mode.

For efficient use of the beam time, a set of on-line physics applications has been developed to support (i) low-energy beam transport (LEBT) tuning, (ii) optimal setting of the multiharmonic buncher (MHB) phases and fields, (iii) beam central trajectory correction in the LEBT, MEBT and cryomodules, (iv) a quadrupole or solenoid scan for profile measurements and evaluation of the rms emittance, (v) a phase scan of the RF cavities, (vi) BPM-based time-of-flight (TOF) measurements to determine the absolute beam energy, and (vii) data processing from a silicon detector for total kinetic energy. The details of the studies have been reported previously [9]. The measured beam parameters, both in transverse and longitudinal phase space, were found to be very close to the design values. Nominal design beam acceleration to 1.46 MeV/u was demonstrated, and peak beam energies of 2.3 MeV/u were achieved. The beam quality was maintained as the lattice transitioned from quadrupole

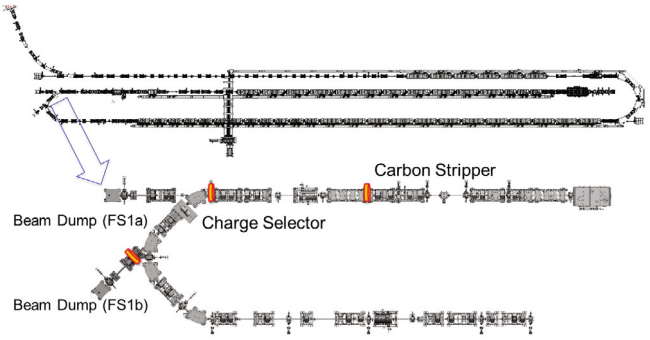

Fig. 8. LS1 and partial FS1 commissioning beamline. The beam was transported to one of two beam bumps in FS1 (FS1a, FS1b).

Fig. 9. Measured beam centroid offsets before (top) and after (bottom) correction by using the orbit response matrix algorithm.

to solenoidal focusing.

The beam is well prepared for the following stages of beam commissioning of the FRIB driver linac. Additionally, high-level applications, diagnostics, and controls for beam commissioning with many independent RF cavities were tested and validated. Fast machine-protection-system interlocks were tested and validated.

Following successful commissioning of the first three cryomodules, the temporary diagnostic station was removed and the first $\beta = 0.085$ cryomodule was installed. The second stage of LS1 commissioning was conducted from February through April of 2019 and comprised the entirety of the LS1 cryomodules, as well as the warm transport sections of LS1 to the beam dumps in FS1, as shown in Fig. 8. The cryogenic section of LS1 is composed of 15 cryomodules with 104 SRF cavities and 39 superconducting solenoid magnets. Four separate ion species ($^{40}Ar^{9+}$, $^{86}Kr^{17+}$, $^{10}Ne^{6+}$, and $^{129}Xe^{26+}$) were accelerated to 20.3 MeV/u by using 14 cryomodules and 99 SRF cavities, with 100% beam current transmission measured through the cryomodules and warm transport section. This latter result was achieved after a beam trajectory offset correction had been made using an orbit response matrix algorithm (see Fig. 9). Two-charge-state beam acceleration through LS1 using krypton beams with charge states 17+ and 18+ was performed with 100% beam transmission demonstrated for each charge species while minimizing the longitudinal phase difference between the different charge states at the location of the charge stripper. A carbon-foil stripper has been used to assist multi-charge-state creation, transport, and beam quality studies in the FS1 beamline prior to installation of the liquid-lithium charge stripper for high-power operation. Stripping efficiency studies have been performed for all four ion species, and comparisons were made to the Baron formula [10]. The results, shown in Fig. 10, indicate that thicker carbon foils are required to reach equilibrium charge-state distributions for the heavier ion species. Three charge states of krypton (33+, 34+, 35+) were subsequently transported through the first 45-degree dipole in the FS1 beamline to the FS1b beam dump with nearly perfect transmission. Additional results of detailed beam dynamic studies have been reported recently [11].

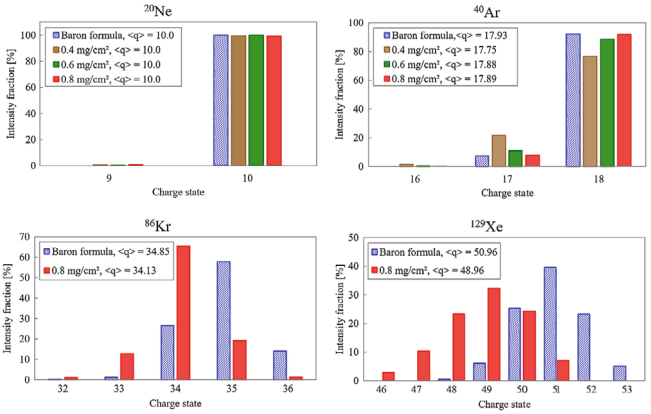

Fig. 10. Measured charge state distributions in FS1 after the carbon-foil charge stripper for various ion species and foil thicknesses with theoretical prediction.

2. Lithium Charge Stripper

Progress is currently being made in off-line commissioning of the liquid-lithium charge-stripper systems for ultimate, high-power operation. Specific milestones have been achieved, including 10-day continuous, unattended operation, electron gun diagnostic construction and commissioning, and measurement of the thickness of the lithium film (see Fig. 11). Operations with the production ion beam are expected in late 2020.

3. Beam Loss Monitoring

Limiting fast and chronic beam losses is essential to support high-power operation. Specific loss-monitoring

Table 2. High-power-beam equivalent modes in LS1 commissioning.

Mode	Ion Species	Peak Current in LS1 (μA)	Pulse Duration (μs)	Repetiton Rate (Hz)	Duty Factor (%)	Average Beam Power at Charge Selector (W)	Average Beam Power in Beam Dump, FS1b (W)
1	Ar	34.3	1000	100	10	31	278
2	Ar	3.2	9995	100	CW	29	260
3	Ar	133.	300	100	3	36	324
4	Ar	133.	6000	5	3	36	324
5	Kr	13.7	1000	100	10	3	138

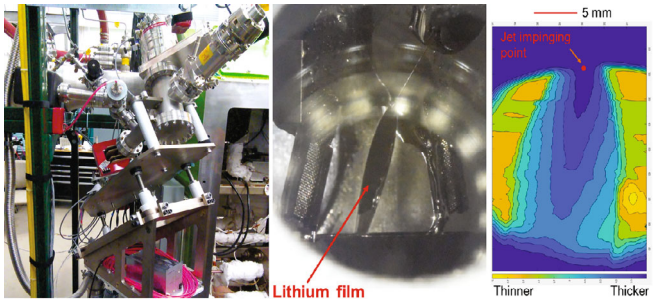

Fig. 11. (Left) Electron gun diagnostic installation on the lithium charge stripper; (middle) image of the liquid lithium film; (right) false color image of the measured lithium film's thickness distribution.

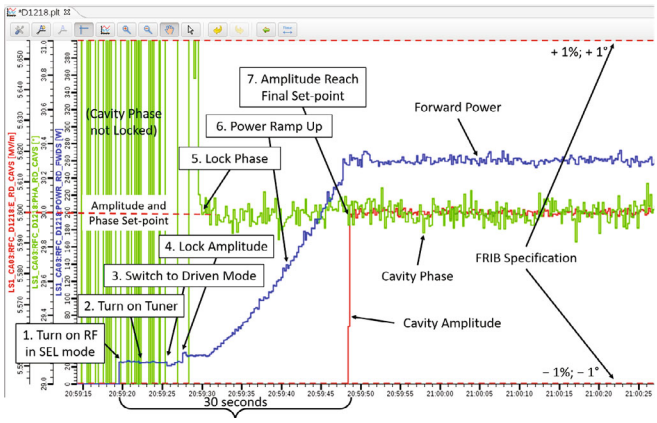

Fig. 12. Temporal sequence for establishing the SRF cavity amplitude and phase tune.

diagnostic systems have been tested and verified during beam commissioning activities. These systems include differential beam current monitoring using BCMs, interceptive halo monitoring rings (HMRs), scintillator-PMT-based neutron monitors and high-pressure ion chambers, and fast thermometry sensors along the cryomodule beam pipe [3]. Differential beam current monitoring across the linac segment has demonstrated sensitivity to better than 0.5 μA on 10-ms averaging time scales, which is currently limited by environmental noise effects at these time scales. Interceptive halo ring monitors, installed between every cryomodule, have demonstrated sensitivities to the pA scale and provide useful feedback for transverse beam envelope tuning at the transition between different symmetry and/or periodicity of transport lattices. Prior to optimization of the beam phase-space matching to the LS1 lattice, appreciable HMR signals were observed in the first three monitors only, at the level of $\sim 2 \times 10^{-4}$ level relative beam loss. After optimization, the signals were reduced to baseline noise levels. Fast losses were generated by mis-steering and defocusing the beam to test the loss sensitivity and the response time of the fast machine protection system. These tests validated the 35-μs beam-mitigation response-time requirement with the beam current monitor, halo monitor ring loss monitor response, and low-level RF monitoring systems.

4. Low-level RF (LLRF) Controls

EPICS-based software and board-level firmware control tools have been developed and implemented to bring all cavities to amplitude and phase lock in parallel. As shown in Fig. 12, the sequence of actions can be accomplished within ∼30 seconds. In practice, all 104 resonators in LS1 can be turned on within ∼2 minutes for routine operation. The achieved amplitude and phase errors ($< \pm 0.1\%_{\text{pk-pk}}$ and $< \pm 0.2°_{\text{pk-pk}}$, respectively) are well within specified requirements ($< 1\%_{\text{pk-pk}}$ and $< \pm 1°_{\text{pk-pk}}$, respectively).

IV. TOWARDS HIGH-POWER OPERATION

Commissioning of the linac systems was performed at a relatively low average beam power. The peak beam currents were in one of several bands around 50, 150, and 250 eμA, with pulse durations of 50–100 μs, and repetition rates up to 100 Hz. Following the conclusion of most linac commissioning and optimization activities, several tests of high beam power operation were conducted. The operational safety envelope was constrained by the average power limits of the beam dumps (135 W for FS1a and 500 W for FS1b). The average powers achieved are

listed in Table 2. With demonstrared CW operation, the FRIB has become the highest energy CW SRF heavy-ion linac in the world.

V. CONCLUSIONS

The front end and the first segment of the FRIB linac, composed of 15 cryomodules, were successfully commissioned with multiple ion beams. A detailed study of the beam parameters demonstrated good consistency with the original design parameters. Four ion-beam species, Ne, Ar, Kr and Xe, were accelerated up to 20.3 MeV/u with 100% transmission and no detectable beam losses. The high quality of the accelerated beam was achieved by fine tuning of both transverse and longitudinal dynamics and successful implementation of beam central trajectory correction by using the optics response matrix method. A high-power equivalent argon beam was accelerated at 3% duty cycle, with a peak current intensity equal to 30% of the ultimate design intensity for the FRIB. The average beam power was limited at this stage by the beam dump power rating. All accelerator hardware showed very reliable operation within the space of design parameters.

ACKNOWLEDGMENTS

This material is based upon work supported by the U.S. Department of Energy, Office of Science, under Cooperative Agreement DE-SC0000661, the State of Michigan, and Michigan State University.

REFERENCES

[1] J. Wei *et al.*, in *Proceedings of HIAT 2012* (Chicago, USA, 2012), p. 8.
[2] G. Machicoane *et al.*, Rev. Sci. Instrum. **87**, 02A743 (2016).
[3] S. Lidia *et al.*, in *Proceedings of IBIC 2015* (Melbourne, Australia, 2015), p. 226.
[4] T. Xu *et al.*, in *Proceedings of SRF 2017* (Lanzhou, China, 2017), p. 345.
[5] V. Ganni *et al.*, in *Proceedings of CEC 2019* (Hartford, USA, 2019), to be published.
[6] H. Ren *et al.*, in *Proceedings of IPAC 2018* (Vancouver, Canada, 2018), p. 1090.
[7] Z. Li *et al.*, in *Proceedings of LINAC 2018* (Beijing, China, 2018), p. 336.
[8] E. Pozdeyev *et al.*, in *Proceedings of IPAC 2018* (Vancouver, Canada, 2018), p. 58.
[9] P. N. Ostroumov *et al.*, Phys. Rev. Accel. Beams **22**, 040101 (2019).
[10] E. Baron *et al.*, Nucl. Instrum. Methods Phys. Res. A **328**, 177 (1993).
[11] P. N. Ostroumov *et al.*, Phys. Rev. Accel. Beams **22**, 080101 (2019).